walls constituting the MWCNT or adjacent walls only are considered in this work, and are given as follows:

2.2.1 The He et al. (2005a, b) Model

In He *et al*. (2005a, b), for an MWCNT the vdW interactive force (q_{ij}) of the i^{th}-wall exerted from the j^{th}-wall of the MWCNT is expressed as $q_{ij} = \overline{C}_{ij}\,\Delta w_{ij}$, in which Δw_{ij} is the relative displacement between the i^{th}- and j^{th}-walls and $\overline{C}_{ij}$ is the vdW interaction coefficient. According to He *et al*. (2005a, b), $\overline{C}_{ij}$ is given in the following form

$$\overline{C}_{ij} = -\left[\frac{1001\pi\varepsilon\sigma^{12}}{3a^4}E_{ij}^{13} - \frac{1120\pi\varepsilon\sigma^{6}}{9a^4}E_{ij}^{7}\right]R_j, \tag{11}$$

where R_j is the mid-surface radius of the j^{th}-wall of the MWCNT, a is the C-C bond length, and a = 0.142 mm, ε = 2.968 meV = 4.7488×10^{-22} J, σ = 0.3407 mm, and

$$E_{ij}^{m} = \left(R_i + R_j\right)^{-m}\int_0^{\pi/2}\left[1 - K_{ij}\cos^2\theta\right]^{-m/2}d\theta, \tag{12}$$

$$K_{ij} = 4R_iR_j\left(R_i + R_j\right)^{-2}. \tag{13}$$

Because the vdW interaction coefficient $\overline{C}_{ij}$ with a unit of nN/(nm)^3 is derived using a cylindrical shell model, it cannot be directly applied to the current nonlocal TBT. The equivalent vdW interaction coefficient C_{ij} with a unit nN/(nm)^2 for a beam model is thus derived as follows (Wu *et al*. 2017)

$$\begin{aligned} 4\int_0^{\pi/2}\overline{C}_{ij}\,\Delta w_{ij}\,R_i\sin^2\theta\,d\theta &= \left(\pi R_i\,\overline{C}_{ij}\right)\Delta w_{ij} \\ &= C_{ij}\,\Delta w_{ij}, \end{aligned} \tag{14}$$

where C_{ij} is obtained as $C_{ij} = \left(\pi R_i\right)\overline{C}_{ij}$.

2.2.2 The Ru model

The main difference between the He *et al*. and Ru models (He *et al*. 2005a, b, Ru 2000) is that in the former the vdW interactive forces are mutually applied between any pair of walls constituting the MWCNT, while in the latter these are mutually applied between adjacent walls only.

In order to have the same definition and sign for the vdW interactive forces used in the He *et al*. model, the authors change the sign for the vdW coefficient of the Ru model, multiply it with a correction factor (πR_{i+1}), and express it in the following form

$$C_{i(i+1)} = C_{(i+1)i} = -\left(\pi R_{i+1}\right)\left[\frac{320\left(2R_i\right)\text{erg}/\left(\text{cm}^2\times\text{nm}\right)}{\left(0.16\Delta^2\right)}\right], \tag{15}$$

where $i = 1 - (N_l - 1)$, Δ = 0.142 nm, and 1 erg = 10^{-7} (N·m). The units of R_i and R_{i+1} are nms, and $C_{kl} = 0$ when $l \neq (k-1)$ or $(k+1)$.

2.3 Hamilton's principle

Hamilton's principle is used to derive the motion equations of the geometrically nonlinear RMVT-based local TBT, and the corresponding energy functional (I_R) for the dynamic version of the geometrically nonlinear RMVT-based local TBT is written in the form of

$$I_R = \int_{t_1}^{t_2} (T - \Pi_R) dt, \tag{16}$$

where T and Π_R denote the kinetic energy and Reissner's strain energy functions, and t is the time variable. $T = \sum_{k=1}^{N_l} T_k$ and $\Pi_R = \sum_{k=1}^{N_l} (\Pi_R)_k$, in which T_k and $(\Pi_R)_k$ are the kinetic energy and Reissner's strain energy functions of the k^{th}-wall CNT, and these are given as follows

$$\begin{aligned} T_k &= \int_0^L \iint_{A_k} (\rho/2)\left[(u_1^k{}_{,t})^2 + (u_2^k{}_{,t})^2 + (u_3^k{}_{,t})^2\right] dA_k\, dx \\ &= \int_0^L \left\{(1/2)\left[m_{k0}(u_{k,t})^2 + m_{k2}(\phi_{k,t})^2 + m_{k0}(w_{k,t})^2\right]\right\} dx, \end{aligned} \tag{17}$$

$$\begin{aligned} (\Pi_R)_k &= \int_0^L \int_{A_k} [\sigma_x^k \varepsilon_x^k + \tau_{xz}^k \gamma_{xz}^k - (\sigma_x^k)^2/(2E_k) - (\tau_{xz}^k)^2/(2k_{ck}G_k)] dA_k\, dx \\ &\quad + \delta_{kN_l} \int_0^L (1/2)\left[k_w (w_k)^2 + k_G (w_{k,x})^2\right] dx \\ &\quad + \int_0^L q_{vdW}^k w_k\, dx + \overline{N}_{k0} u_{k0} - \overline{N}_{kL} u_{kL} + \overline{M}_{k0} \phi_{k0} - \overline{M}_{kL} \phi_{kL} - \overline{V}_{k0} w_{k0} + \overline{V}_{kL} w_{kL} \\ &= \int_0^L \left\{N_k u_{k,x} + (N_k/2)(w_{k,x})^2 - \left[(N_k)^2/(2A_k E_k)\right] + M_k \phi_{k,x}\right. \\ &\quad \left. - \left[(M_k)^2/(2E_k I_k)\right] + Q_k(\phi_k - w_{k,x}) - \left[(Q_k)^2/(2k_{ck} G_k A_k)\right]\right\} dx \\ &\quad + \delta_{kN_l} \int_0^L (1/2)\left[k_w (w_k)^2 + k_G (w_{k,x})^2\right] dx \\ &\quad + \int_0^L q_{vdW}^k w_k\, dx + \overline{N}_{k0} u_{k0} - \overline{N}_{kL} u_{kL} + \overline{M}_{k0} \phi_{k0} - \overline{M}_{kL} \phi_{kL} - \overline{V}_{k0} w_{k0} + \overline{V}_{kL} w_{kL}, \end{aligned} \tag{18}$$

in which ρ is the mass density of the CNT, and the inertias m_{k0} and m_{k2} are defined as $m_{k0} = \iint_{A_k} \rho\, dA_k$ and $m_{k2} = \iint_{A_k} \rho\, z^2\, dA_k$. k_w and k_G are the Winkler stiffness and shear modulus of the surrounding elastic medium, respectively, and $\overline{N}_{k0}, \overline{N}_{kL}$, $\overline{M}_{k0}, \overline{M}_{kL}$, $\overline{V}_{k0}$ and $\overline{V}_{kL}$ denote the applied axial forces, moments and shear forces of the k^{th}-wall CNT at the edges, and are shown in Fig. 1. δ_{kl} is the Dirac delta function, in which $\delta_{kl} = 1$ when $k = l$, while $\delta_{kl} = 0$ when $k \neq l$. q_{vdW}^k denotes the total vdW interactive forces of the k^{th}-wall CNT exerted from other walls, respectively, the positive direction of which is defined to be downward. The term $q_{vdW}^k\, \delta w_k$ is given as follows

$$q_{vdW}^{k}\ \delta w_k = \left[\sum_{\substack{l=1 \\ (l\neq k)}}^{N_l} \left(C_{kl} w_l\right) - \left(\sum_{\substack{l=1 \\ (l\neq k)}}^{N_l} C_{kl} \right) w_k \right] \delta w_k, \tag{19}$$

where C_{kl} denotes the vdW interaction coefficient. For an MWCNT, C_{kl} of the He *et al*. and Ru models are given in Eqs. (11)-(14) and (15), respectively (He *et al*. 2005a, b, Ru 2000).

Performing the first-order variation of the above-mentioned energy functional (I_R), using integration by parts, and then imposing the stationary principle of the above-mentioned energy functional (i.e., $\delta I_r = 0$), the authors obtain the motion equations of the geometrically nonlinear RMVT-based local TBT and the possible boundary conditions as follows:

Motion equations in the interior domain of the k^{th}-wall CNT ($0 < x < L$)

$$\delta u_k :\ -N_{k,x} = -m_{k0}\, u_{k,tt}, \tag{20}$$

$$\delta w_k :\ Q_{k,x} - N_{k,x}\, w_{k,x} - N_k\, w_{k,xx} = -q_{vdW}^{k} - \delta_{kN_l}\left(k_w\, w_k - k_G\, w_{k,xx}\right) - m_{k0}\, w_{k,tt}, \tag{21}$$

$$\delta \phi_k :\ -M_{k,x} + Q_k = -m_{k2}\, \phi_{k,tt}, \tag{22}$$

$$\delta N_k :\ N_k - A_k E_k \left[u_{k,x} + (1/2)\left(w_{k,x}\right)^2\right] = 0, \tag{23}$$

$$\delta M_k :\quad M_k - E_k\, I_k\, \phi_{k,x} = 0, \tag{24}$$

$$\delta Q_k :\ Q_k - k_{ck}\, G_k A_k \left(\phi_k - w_{k,x}\right) = 0, \tag{25}$$

where $k = 1, 2, \ldots, N_l$.

Possible boundary conditions at the edges of the MWCNT

At $x = 0$, either

$$u_{k0} = \overline{u}_{k0} \quad \text{or} \quad N_{k0} = \overline{N}_{k0}, \tag{26a}$$

either

$$w_{k0} = \overline{w}_{k0} \quad \text{or} \quad Q_{k0} - N_{k0}\left(w_{k0,x}\right) - \delta_{kN_l} k_G \left(w_{k0,x}\right) = \overline{V}_{k0}, \tag{26b}$$

either

$$\phi_{k0} = \overline{\phi}_{k0} \quad \text{or} \quad M_{k0} = \overline{M}_{k0}; \tag{26c}$$

At $x = L$, either

$$u_{kL} = \overline{u}_{kL} \quad \text{or} \quad N_{kL} = \overline{N}_{kL}, \tag{27a}$$

either

$$w_{kL} = \overline{w}_{kL} \quad \text{or} \quad Q_{kL} - N_{kL}\left(w_{kL,x}\right) - \delta_{kN_l} k_G \left(w_{kL,x}\right) = \overline{V}_{kL}, \tag{27b}$$

either

$$\phi_{kL} = \overline{\phi}_{kL} \quad \text{or} \quad M_{kL} = \overline{M}_{kL}. \tag{27c}$$

3. The geometrically nonlinear RMVT-based nonlocal TBT

3.1 Eringen's nonlocal constitutive relations

In the nonlocal elasticity theory, the stress components induced at a particular material point of the loaded elastic body will depend on the strain components induced at all the material points of the continuum, due to the effects of the small length scale. According to ENET, the nonlocal constitutive behavior of an elastic body can be written as

$$\left(1 - \mu \nabla^2\right)\sigma_{ij} = c_{ijkl}\, \varepsilon_{kl}, \tag{28}$$

where μ denotes the nonlocal parameter, and $\mu = (e_0 a_0)^2$, in which a_0 is the internal characteristic length and e_0 is a constant used to adjust the nonlocal continuum model by matching its results with some of the reliable results obtained by experiments or other models. c_{ijkl} are the stiffness coefficients of the elastic beam-like solid, and σ_{ij} and ε_{kl} are the stress and strain components, respectively.

Using Eq. (28), the author can write the constitutive equations of the k^{th}-wall CNT for the nonlocal Timoshenko beam theory, as follows

$$\sigma_x^k - \mu \sigma_{x,xx}^k = E_k\, \varepsilon_x^k, \tag{29}$$

$$\tau_{xz}^k - \mu \tau_{xz,xx}^k = k_{ck}\, G_k\, \gamma_{xz}^k, \tag{30}$$

Using Eqs. (29) and (30) in conjunction with Eqs. (9a)-(9c), we can express the axial force, bending moment and shear force resultants of the k^{th}-wall CNT in terms of the generalized displacement components as

$$N_k - \mu N_{k,xx} = A_k E_k \left[u_{k,x} + (1/2)\left(w_{k,x}\right)^2\right], \tag{31}$$

$$M_k - \mu M_{k,xx} = E_k I_k\, \phi_{k,x}, \tag{32}$$

$$Q_k - \mu Q_{k,xx} = k_{ck}\, G_k\, A_k \left(\phi_k - w_{k,x}\right). \tag{33}$$

Eqs. (31)-(33) combined with Eqs. (20)-(22) constitute the set of motion equations of the geometrically nonlinear RMVT-based nonlocal TBT, and Eqs. (26a)-(26c) and (27a)-(27c) are the possible boundary conditions at the edges. These equations constitute the strong formulation of the dynamic version of the geometrically nonlinear nonlocal TBT, and are a well-posed eigen-value problem for the nonlinear free vibration analysis of an embedded MWCNT with different

boundary conditions.

4. Applications

In this section, the primary variables are expressed as a harmonic function in the time domain, and then the DQ method (Du *et al*. 1994, Wu and Lee 2001) is used to construct the weighting coefficients for the first- and higher-order derivatives of the primary variables in the spatial (x) domain, such that

$$\left.\frac{\partial F^r(x,t)}{\partial x^r}\right|_{x=x_i} = \left(\sum_{j=1}^{n_p} A_{ij}^{(r)} F_j\right) e^{i\omega t}, \tag{34}$$

where $r \geq 1$, $F_j = (u_k)_j$, $(w_k)_j$, $(\phi_k)_j$, $(N_k)_j$, $(M_k)_j$ and $(Q_k)_j$. ω denotes the natural frequency of the embedded MWCNT.

Applying the DQ formulae (i.e., Eq. (34)) to the strong formulation for the nonlinear free vibration problem of an embedded MWCNT based on the geometrically nonlinear RMVT-based nonlocal TBT, the authors obtain a set of simultaneous nonlinear algebraic equations, in which four different boundary conditions will be considered, such as the simple-simple (SS), clamped-clamped (CC) and clamped-simple (CS) and clamped-free (CF) supports.

Applying the DQ formulae to the motion equations at the sampling nodes in the interior domain, and satifying the associated boundary conditions at two edges, we finally obtain a set of $6(n_p - 1)N_l$ simultaneously algebraic equations in terms of $6(n_p - 1)N_l$ unknowns, which represents a standard nonlinear eigenvalue problem. Because a direct iterative method is used to solve these nonlinear equations, they are rewritten in the matrix form as follows

$$\left(\begin{bmatrix} \mathbf{K}_{11}^{(m)} & \mathbf{K}_{12}^{(m)} \\ \mathbf{K}_{21}^{(m)} & \mathbf{K}_{22}^{(m)} \end{bmatrix} + \begin{bmatrix} \mathbf{G}_{11}^{(m-1)} & \mathbf{0} \\ \mathbf{G}_{21}^{(m-1)} & \mathbf{0} \end{bmatrix} - \omega^2 \begin{bmatrix} \mathbf{M}_{11}^{(m)} & \mathbf{0} \\ \mathbf{0} & \mathbf{0} \end{bmatrix}\right) \begin{Bmatrix} \mathbf{X}_1^{(m)} \\ \mathbf{X}_2^{(m)} \end{Bmatrix} = \begin{Bmatrix} \mathbf{0} \\ \mathbf{0} \end{Bmatrix}, \tag{35}$$

where the superscript m denotes the m^{th} iteration. The coefficients $\mathbf{G}_{11}^{(m-1)}$ and $\mathbf{G}_{21}^{(m-1)}$ are in terms of the determined variables $\mathbf{X}_1^{(m-1)}$ and $\mathbf{X}_2^{(m-1)}$, and let $\mathbf{G}_{11}^{(0)} = \mathbf{G}_{21}^{(0)} = \mathbf{0}$, which means the linear solutions will be used as the initial guess of the unknowns to obtain the nonlinear ones, i.e., the convergent solutions obtained from the direct iterative method with an allowable error $\in_\alpha$ less than 10^{-5}, in which the allowable error $\in_\alpha$ is defined as $\in_\alpha = \sqrt{\left(\mathbf{X}^{(m)} - \mathbf{X}^{(m-1)}\right) \bullet \left(\mathbf{X}^{(m)} - \mathbf{X}^{(m-1)}\right)} / \sqrt{\left(\mathbf{X}^{(m)}\right) \bullet \left(\mathbf{X}^{(m)}\right)}$, in which the symbol , $\bullet$, denotes the inner product operation for two vectors, and $\mathbf{X}^{(m)} = \left\{\mathbf{X}_1^{(m)} \ \mathbf{X}_2^{(m)}\right\}^T$.

A matrix partition process and a direct iterative method are performed to solve the natural frequencies of an embedded MWCNT with various boundary conditions. From the second equation in Eq. (35), one can obtain

$$\mathbf{X}_2^{(m)} = -\left(\mathbf{K}_{22}^{(m)}\right)^{-1} \left(\mathbf{K}_{21}^{(m)} + \mathbf{G}_{21}^{(m-1)}\right) \mathbf{X}_1^{(m)}. \tag{36}$$

Using Eq. (36), the authors can condense Eq. (35) in the following form of

$$\left[\left(\mathbf{K}_{11}^{(m)}+\mathbf{G}_{11}^{(m-1)}\right)-\mathbf{K}_{12}^{(m)}\left(\mathbf{K}_{22}^{(m)}\right)^{-1}\left(\mathbf{K}_{21}^{(m)}+\mathbf{G}_{21}^{(m-1)}\right)-\omega^2\,\mathbf{M}_{11}^{(m)}\right]\mathbf{X}_1^{(m)}=\mathbf{0}. \tag{37}$$

Eq. (37) represents a standard eigenvalue problem, and a nontrivial solution of this exists if the determination of the coefficient matrix vanishes. The natural frequencies can thus be obtained by

$$\left|\left(\mathbf{K}_{11}^{(m)}+\mathbf{G}_{11}^{(m-1)}\right)-\mathbf{K}_{12}^{(m)}\left(\mathbf{K}_{22}^{(m)}\right)^{-1}\left(\mathbf{K}_{21}^{(m)}+\mathbf{G}_{21}^{(m-1)}\right)-\omega^2\,\mathbf{M}_{11}^{(m)}\right|=\mathbf{0}. \tag{38}$$

Once Eq. (38) is solved, the corresponding eigenvectors, which consist of nodal generalized displacement and force resultant components for each wall, can thus be obtained. In this work, the authors approximately scaled up this eigenvector such that the maximum transverse displacement of the innermost wall is equal to a given vibration amplitude $(W_1)_{\max}$, which means the authors let $w_1(x = 0.5L) = (W_1)_{\max}$ in the SS and CC cases, while $w_1(x = 0.57L) = (W_1)_{\max}$ in the CS cases and $w_1(x = L) = (W_1)_{\max}$ in the CF cases. Using the scaled up eigenvector to determine the nonlinear coefficient matrices, i.e., $\mathbf{G}_{11}^{(m-1)}$ and $\mathbf{G}_{21}^{(m-1)}$, a new eigenvalue and eigenvector can be thus obtained by using the updated eigenvalue system equations (i.e., Eq. (35)). Using this iterative process, the authors can obtain the convergent solutions of the natural frequencies of the embedded MWCNT until the relative error between the natural frequencies (ω) of m^{th} and $(m\text{-}1)^{\text{th}}$ iterations and that between the mean-square norm of the scaled up displacement vector ($\mathbf{X}_1$)of m^{th} and $(m - 1)^{\text{th}}$ iterations are less than an allowable error, which is 10^{-5} in this work.

5. Illustrative examples

5.1 Non-embedded DWCNTs

The linear vibration characteristics of a non-embedded DWCNT with combinations of simply supported and clamped boundary conditions have been examined by Ke *et al*. (2009) using the PVD-based nonlocal TBT, in which the vdW interaction of Ru's model was used. This issue was also studied by Ehteshami and Hajabasi (2011) and Shakouri *et al*. (2009) using the PVD-based nonlocal EBBT, as well as by Wang *et al*. (2006a) using the PVD-based nonlocal EBBT and TBT. These solutions of the frequency parameters of the DWCNT with assorted boundary conditions are used for assessing the accuracy of the current RMVT-based nonlocal TBT.

Table 1 shows the current DQ solutions of RMVT-based nonlocal TBT for the first three lowest frequency parameters ($\overline{\omega}$) of a DWCNT with different boundary conditions, in which μ = 0 and 1.96 nm^2, $\overline{\omega}=\sqrt[4]{\rho A_t L^4 \omega/(E I_t)}$, $A_t = A_1 + A_2$, $I_t = I_1 + I_2$, n_p = 15, and the values of k_{ck} (k = 1 and 2 are given using the formula from Cowper (1966).

The geometric parameters and material properties are the same as those used in Ke *et al*. (2009), which are $h_1 = h_2$ = 0.35 nm, L = 14 nm, $R_1 = R_2$ = 0.35 nm : 0.7 nm, E = 1000 GPa, υ = 0.25, ρ = 2.3×10^3 kg/m^3.

It can be seen in Table 1 that the solutions of the first three lowest frequency parameters of the non-embedded DWCNT obtained using the current RMVT-based nonlocal TBT agree closely with the solutions of Ke *et al*. (2009) and Wang *et al*. (2006a) obtained using the PVD-based nonlocal TBT. These solutions for the first mode are lower than the solutions obtained using the PVD-based nonlocal EBBT by about 0.64%, 1.3%, 3.1% and 5.2% for the cases of CF, SS, CS and CC edges,

Table 1 The DQ solutions of RMVT- based nonlocal TBT for the first three lowest frequency parameters ($\overline{\omega}$) of a DWCNT with various boundary conditions, and without foundation models

BCs	Theories	$\mu = 0$ (nm)^2			$\mu = 1.96$ (nm)^2		
		1st mode	2nd mode	3rd mode	1st mode	2nd mode	3rd mode
SS	[a]Wang *et al*. (2006a)	3.1410	6.2650	9.2756	NA	NA	NA
	Ehteshami and Hajabasi (2011)	3.141	6.265	9.276	3.068	5.770	7.976
	Shakouri *et al*. (2009)	3.1413	6.2735	9.3476	3.0683	5.7753	8.0060
	[b]Wang *et al*. (2006a)	3.0662	6.0378	8.5758	NA	NA	NA
	Ke *et al*. (2009)	3.099	NA	NA	3.027	NA	NA
	[c]Current linear	3.099	5.977	8.531	3.027	5.501	7.288
	[d]Current linear	3.099	5.974	8.513	3.027	5.499	7.281
CS	[a]Wang *et al*. (2006a)	3.9253	7.0355	9.9811	NA	NA	NA
	Ehteshami and Hajabasi (2011)	3.925	7.035	9.981	3.819	6.444	8.557
	Shakouri *et al*. (2009)	3.93	7.05	10.09	3.82	6.45	8.60
	[b]Wang *et al*. (2006a)	3.8598	6.7185	9.2148	NA	NA	NA
	Ke *et al*. (2009)	3.802	NA	NA	3.701	NA	NA
	[c]Current linear	3.802	6.539	8.954	3.702	5.997	7.631
	[d]Current linear	3.802	6.534	8.934	3.702	5.994	7.622
CC	Ehteshami and Hajabasi (2011)	4.726	7.796	10.654	4.590	7.105	9.123
	Shakouri *et al*. (2009)	4.73	7.82	10.82	4.59	7.12	9.19
	Ke *et al*. (2009)	4.482	NA	NA	4.359	NA	NA
	[c]Current linear	4.484	7.054	9.344	4.361	6.446	7.944
	[d]Current linear	4.483	7.047	9.322	4.360	6.441	7.935
CF	Ehteshami and Hajabasi (2011)	1.875	4.690	7.797	1.879	4.544	7.111
	Shakouri *et al*. (2009)	1.88	4.69	7.82	1.88	4.55	7.13
	[c]Current linear	1.863	4.502	7.021	1.867	4.359	6.537
	[d]Current linear	1.863	4.501	7.021	1.867	4.358	6.532

[a] The solutions are obtained by Wang *et al*. (2006a) using the PVD-based nonlocal EBBT
[b] The solutions are obtained by Wang *et al*. (2006a) using the PVD-based nonlocal TBT
[c] The solutions are obtained using the current RMVT-based nonlocal TBT and the vdW interaction model of Ru (2000)
[d] The solutions are obtained using the current RMVT-based nonlocal TBT and vdW interaction model of He *et al*. (2005a, b)

respectively, and these deviations between the frequency parameters obtained using the nonlocal EBBT and TBT become greater, i.e. the effect of shear deformation increases, for the higher modes. The effect of shear deformation will soften the gross stiffness of the DWCNT, and the effect of this on the frequency parameters of the DWCNT with different boundary conditions follow the order of CC > CS > SS > CF. Moreover, the results also show the solutions of the lowest frequency parameters of the DWCNT obtained using the vdW interaction models of Ru and He *et al*. are almost identical to each other.

For the future study purposes, the vdW coefficients of a five-walled CNT obtained using the

Table 2 vdW interaction coefficients C_{kl} (nN/nm^2) between the k^{th} and l^{th} walls of a five-walled CNT using the modified formulae of He *et al*. and Ru

	No. layers (N_l)	$l = 1$	$l = 2$	$l = 3$	$l = 4$	$l = 5$
$k = 1$	He *et al*. (2005a, b)	0	-92.3317	3.1698	0.3386	0.0690
	Ru (2000)	0	-152.6860	0	0	0
$k = 2$	He *et al*. (2005a, b)	-92.3317	0	-161.4667	5.0062	0.5107
	Ru (2000)	-152.6860	0	-458.0580	0	0
$k = 3$	He *et al*. (2005a, b)	3.1698	-161.4667	0	-228.7969	6.7941
	Ru (2000)	0	-458.0580	0	-916.1161	0
$k = 4$	He *et al*. (2005a, b)	0.3386	5.0062	-228.7969	0	-295.5899
	Ru (2000)	0	0	-916.1161	0	-1526.8601
$k = 5$	He *et al*. (2005a, b)	0.0690	0.5107	6.7941	-295.5899	0
	Ru (2000)	0	0	0	-1526.8601	0

modified formulae of He *et al*. (2005a, b) and Ru (2000) are listed in Table 2, in which the thickness of each wall are $h_1 = h_2 = h_3 = h_4 = h_5 = 0.35$ nm and the mid-surface radii of each wall are $R_1 : R_2 : R_3 : R_4 : R_5 = 0.35$ nm (1 : 2 : 3 : 4 : 5).

5.2 Embedded TWCNTs

In this section, the authors investigate the nonlinear vibration characteristics of embedded and non-embedded TWCNTs with SS and CC boundary conditions, in which the vdW interaction model of He *et al*. (2005a, b), Cowper's shear stress correction factor formula, and a Pasternak-type foundation model are used. The material properties of the CNT are $E = 1000$ GPa, $\upsilon = 0.25$, $\rho = 2300$ kg/m^3, and the effective thickness of each individual wall is $h_k = 0.35$ nm. A frequency parameter ratio between the nonlinear solutions and linear solutions for the i^{th} vibration mode is defined as $R_{\omega_i} = (\omega_i)_{nl} / (\omega_i)_l$. As mentioned before, the nonlinear solutions of the lowest frequency parameters are dependent upon the amplitude of the vibration mode, such that in the analysis the nonlinear solutions of frequency parameters will be obtained in association with a given value of the maximum modal deflection at $x = 0.5L$ of the innermost wall, i.e., $(W_1)_{max}$, for the SS and CC edges.

Fig. 3 shows variations of the frequency parameter ratios of the first mode ($(\omega_1)_{nl}/(\omega_1)_l$) of the non-embedded SW, DW and TW CNTs with the maximum modal deflection ($(W_1)_{max}$) for the cases of SS and CC edges, in which $\mu = 1$ (nm)^2, $L = 20$ nm, as well as $R_1 = 0.35$ nm $R_1 : R_2 = 0.35$ nm : 0.7 nm and $R_1 : R_2 : R_3 = 0.35$ nm : 0.7 nm : 1.05 nm for the SW, DW and TW CNTs, respectively. It is shown that the frequency parameter ratio increases when the value of the maximum modal deflection becomes greater. The geometrically nonlinear effect on the frequency parameters of non-embedded MWCNTs with different boundary conditions is SS > CC and SWCNT > DWCNT > TWCNT, in which the symbol ">" means more significant.

Fig. 4 shows variations of the frequency parameter ratios of the first mode of the non-embedded TWCNTs with the length-to-radius ratio (L/R_3) for the cases of SS and CC edges, in which $(W_1)_{max} = 0.6$ nm, $\mu = 0$, 1 and 2 (nm)^2 and $L/R_3 = 7 - 50$. It can be seen in Fig. 4 that the geometrically nonlinear effect will stiffen the TWCNT, such that the frequency parameter ratios

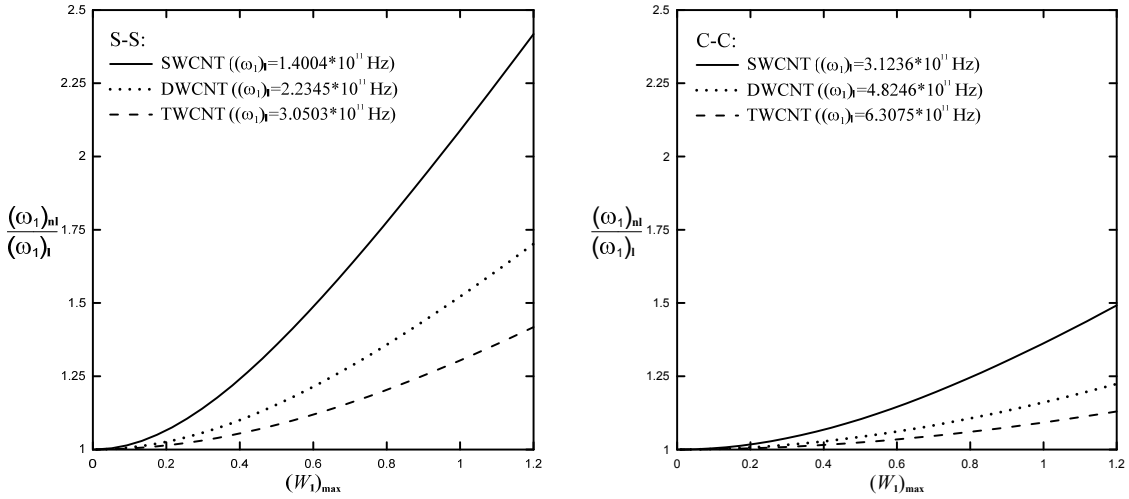

Fig. 3 Variations of the frequency parameter ratios of the first mode of non-embedded SW, DW and TW CNTs with maximum modal deflection: (a) SS; (b) CC supports

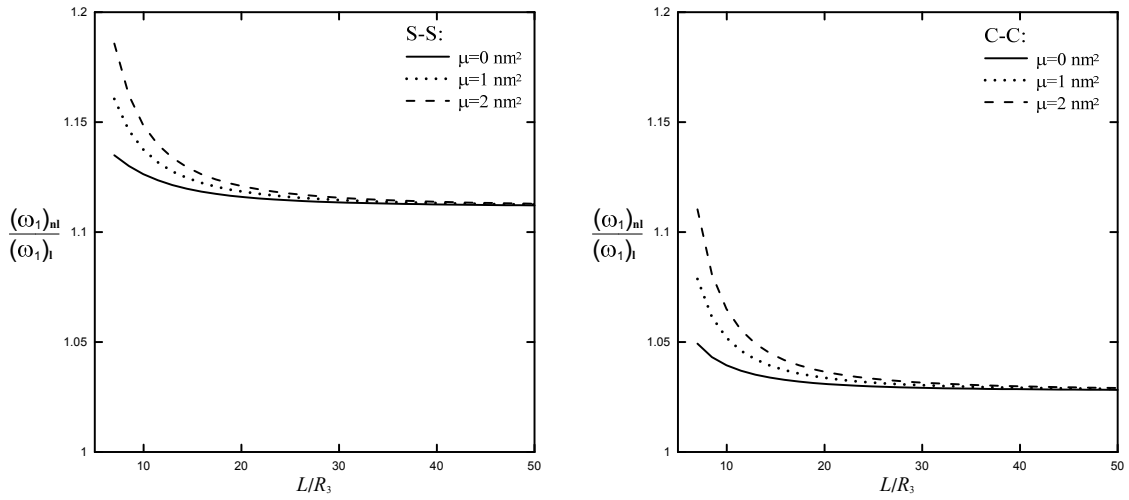

Fig. 4 Variations of the frequency parameter ratios of the first mode of non-embedded TWCNTs with the length-to-radius ratio: (a) SS; (b) CC supports

are always larger than 1, and this effect on the frequency parameters of the non-embedded TWCNT with short length is more significant than that seen on the one with long length.

Figs. 5 and 6 show variations of the frequency parameter ratios of the first mode of the embedded TWCNTs with the dimensionless Winkle spring stiffness (K_w) and the dimensionless shear modulus of the surrounding medium (K_G) for the cases of SS and CC edges, in which L = 20 nm, $(W_1)_{max}$ = 0.6 nm, μ = 0, 1 and 2 (nm)^2, as well as K_G = 0 and K_w = 100 in Figs. 5 and 6, respectively. It can be seen in Figs. 5 and 6 that the frequency parameter ratio decreases when the

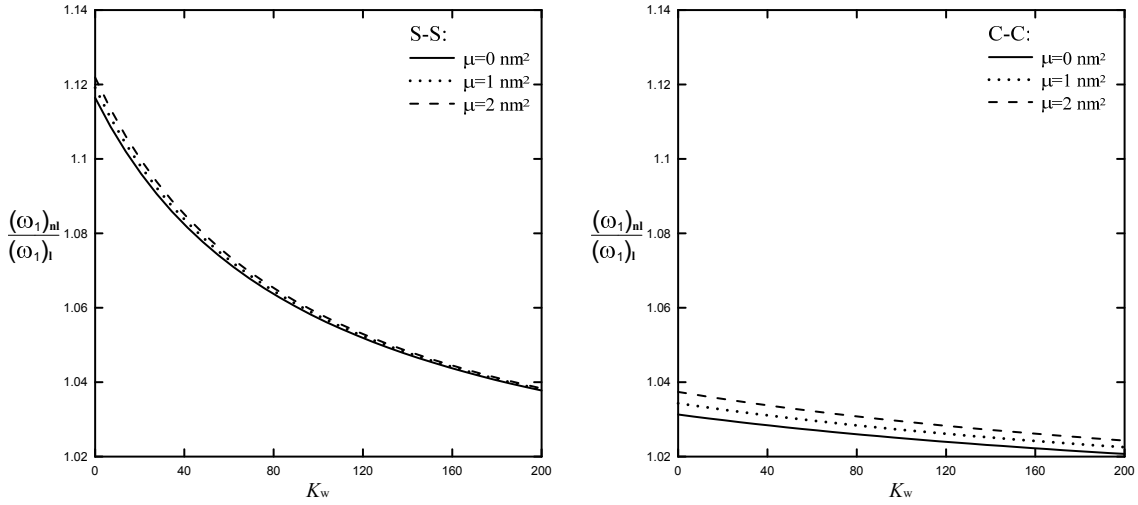

Fig. 5 Variations of the frequency parameter ratios of the first mode of embedded TWCNTs with the dimensionless Winkler stiffness: (a) SS; (b) CC supports

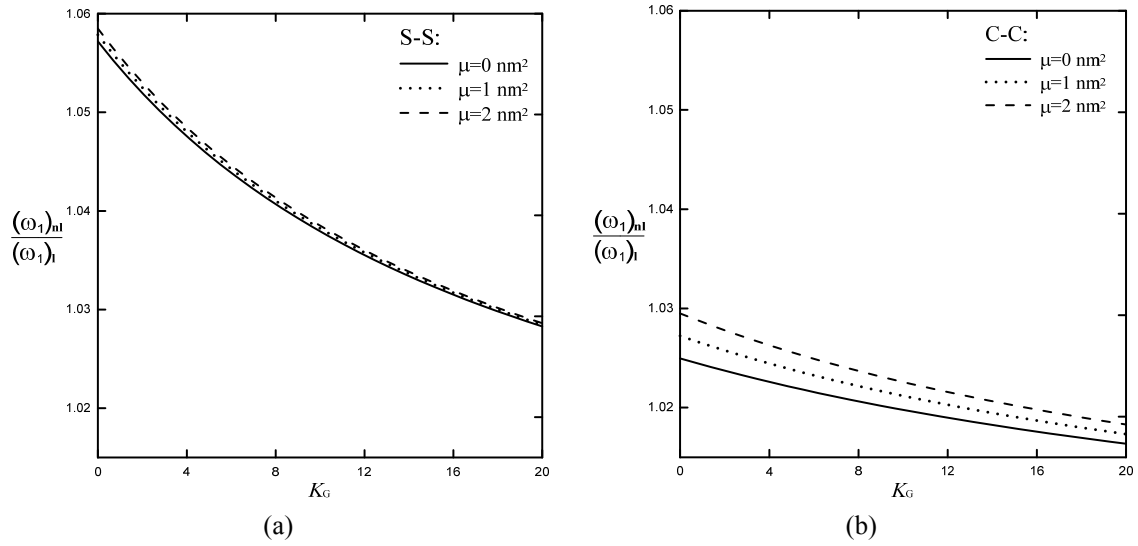

Fig. 6 Variations of the frequency parameter ratios of the first mode of embedded TWCNTs with the dimensionless shear modulus of the surrounding medium: (a) SS; (b) CC supports

values of K_w and K_G become greater. In contrast, the frequency parameter ratio increases when the nonlocal parameter becomes greater.

6. Conclusions

In this article the authors developed the RMVT-based nonlocal TBT for the nonlinear free

vibration analysis of embedded and non-embedded MWCNTs with various boundary conditions. The strong formulation of the RMVT-based nonlocal TBT and its associated possible boundary conditions for a typical individual wall are derived using the Hamilton principle, in which the generalized displacement (i.e., in- and out-of-surface displacement and total rotation) and generalized force (axial force, shear force and bending moment) variables of each wall are regarded as the primary variables, which differs from the PVD-based nonlocal TBT, in which the generalized displacement components of each individual wall are considered as the primary variables only. Two different formulae of vdW interactive forces, which are the He *et al*. and Ru models, derived from a nonlocal cylindrical shell model are modified to be suitable for the nonlocal beam model, and it is happy to see that the frequency parameters of MWCNTs obtained using the current RMVT-based nonlocal TBT combined with these two different models yield the identical results each other. The vdW interaction coefficients of a five-walled CNT obtained using the He *et al*. and Ru models are tabulated for future reference. In the numerical examples, it is shown that the solutions of the current RMVT-based nonlocal TBT converge rapidly and their convergent solutions are in excellent agreement with the accurate ones available in the literature. The results also show that the shear deformation effects on the frequency parameters of the MWCNTs for higher modes are more significant than those on the frequency parameters of MWCNTs for the first mode. The shear deformation effects will soften the gross stiffness of the MWCNTs, such that the frequency parameters of the MWCNTs obtained using the nonlocal TBT are always lower than those obtained using the nonlocal EBBT. The geometrical nonlinear effects on the frequency parameters of the MWCNTs become significant when the maximum amplitude of the modal shape of the MWCNTs approach the total thickness of the MWCNTs. Moreover, the different boundary conditions, nonlocal parameter, aspect ratio, and the Winkler stiffness and shear modulus of the surrounding medium significantly affect the free vibration behaviors of the embedded MWCNT.

Acknowledgments

This work was supported by the Ministry of Science and Technology of Republic of China through Grant MOST 103-2221-E-006-064-MY3.

References

Aissani, K., Bouiadjra, M.B., Ahouel, M. and Tounsi, A. (2015), "A new nonlocal hyperbolic shear deformation theory for nanobeams embedded in an elastic medium", *Struct. Eng. Mech., Int. J.*, **55**(4), 743-763.

Ansari, R. and Ramezannezhad, H. (2011), "Nonlocal Timoshenko beam model for the large-amplitude vibrations of embedded multiwalled carbon nanotubes including thermal effects", *Physica E*, **43**(6), 1171-1178.

Ansari, R. and Sahmani, S. (2012), "Small scale effect on vibrational response of single-walled carbon nanotubes with different boundary conditions based on nonlocal beam models", *Commun. Nonlin. Sci. Numer. Simul.*, **17**(4), 1965-1979.

Aydogdu, M. (2009), "A general nonlocal beam theory: Its application to nanobeam bending, buckling and vibration", *Physica E*, **41**(9), 1651-1655.

Behera, L. and Chakraverty, S. (2015), "Application of differential quadrature method in free vibration analysis of nanobeams based on various nonlocal theories", *Comput. Math. Appl.*, **69**(12), 1444-1462.

Behera, L. and Chakraverty, S. (2016), "Recent researches on nonlocal elasticity theory in the vibration of carbon nanotubes using beam models: A review", *Arch. Comput. Methods Eng.* DOI: 10.1007/s11831-016-9179-y

Bianco, A., Kostarelos, K. and Prato, M. (2005), "Applications of carbon nanotubes in drug delivery", *Current Opinion Chem. Biology*, **9**, 674-679.

Carrera, E. (2000), "An assessment of mixed and classical theories on global and local responses of multilayered orthotropic plates", *Compos. Struct.*, **50**(2), 183-198.

Carrera, E. (2004), "Assessment of theories for free vibration analysis of homogeneous and multilayered plates", *Shock Vib.*, **11**(3-4), 261-270.

Chen, W.X., Tu, J.P., Wang, L.Y., Gan, H.Y., Xu, Z.D. and Zhang X.B. (2003), "Tribological application of carbon nanotubes in a metal-based composite coating and composites", *Carbon*, **41**, 215-222.

Cowper, G. (1966), "The shear coefficient in Timoshenko's beam theory", *J. Appl. Mech.*, **33**(2), 335-340.

Datsyuk, V., Kalyva, M., Papagelis, K., Parthenios, J., Tasis, D., Siokou, A., Kallitsis, I. and Galiotis, C. (2008), "Chemical oxidation of multiwalled carbon nanotubes", *Carbon*, **46**, 833-840.

De Volder, M.F.L., Tawfick, S.H., Baughman, R.H. and Hart, A.J. (2013), "Carbon nanotubes: present and future commercial applications", *Sci.*, **339**, 535-539.

Du, H., Lim, M. and Lin, R. (1994), "Application of generalized differential quadrature method to structural problems", *Int. J. Numer. Methods Eng.*, **37**(11), 1881-1896.

Ebrahimi, F. and Barati, M.R. (2016a), "Analytical solution for nonlocal buckling characteristics of higher-order inhomogeneous nanosize beams embedded in elastic medium", *Adv. Nano Res., Int. J.*, **4**(3), 229-249.

Ebrahimi, F. and Barati, M.R. (2016b), "A nonlocal higher-order refined magneto-electro-viscoelastic beam model for dynamic analysis of smart nanostructures", *Int. J. Eng. Sci.*, **107**, 183-196.

Ebrahimi, F. and Barati, M.R. (2016c), "Dynamic modeling of a thermo-piezo-electrically actuated nanosize beam subjected to a magnetic field", *Appl. Phys. A*, **122**, 451 (18 pages).

Ebrahimi, F. and Barati, M.R. (2018), "Vibration analysis of smart piezoelectrically actuated nanobeams subjected to magneto-electrical field in thermal environment", *J. Vib. Control*, **24**(3), 549-564.

Ebrahimi, F. and Salari, E. (2015a), "Nonlocal thermo-mechanical vibration analysis of functionally graded nanobeams in thermal environment", *Acta Astronautica*, **113**, 29-50.

Ebrahimi, F. and Salari, E. (2015b), "Thermo-mechanical vibration analysis of a single-walled carbon nanotube embedded in an elastic medium based on higher-order shear deformation beam theory", *J. Mech. Sci. Technol.*, **29**(9), 3797-3803.

Ebrahimi, F. and Salari, E. (2015c), "Size-dependent free flexural vibrational behavior of functionally graded nanobeams using semi-analytical differential transform method", *Compos. Part B: Eng.*, **79**, 156-169.

Ebrahimi, F. and Salari, E. (2016), "Effect of various thermal loadings on buckling and vibrational characteristics of nonlocal temperature-dependent functionally graded nanobeams", *Mech. Adv. Mater. Struct.*, **23**(12), 1379-1397.

Ebrahimi, F. and Shafiei, N. (2016), "Application of Eringen's nonlocal elasticity theory for vibration analysis of rotating functionally graded nanobeams", *Smart Struct. Syst., Int. J.*, **17**(5), 837-857.

Ebrahimi, F., Ghadiri, M., Salari, E., Hoseini, S.A.H. and Shaghaghi, G.R. (2015), "Application of the differential transformation method for nonlocal vibration analysis of functionally graded nanobeams", *J. Mech. Sci. Technol.*, **29**(3), 1207-1215.

Ehteshami, H. and Hajabasi, M.A. (2011), "Analytical approaches for vibration analysis of multi-walled carbon nanotubes modeled as multiple nonlocal Euler beams", *Physica E*, **44**(1), 270-285.

Eltaher, M.A., Khater, M.E. and Emam, S.A. (2016), "A review on nonlocal elastic models for bending, buckling, vibrations, and wave propagation of nanoscale beams", *Appl. Math. Modell.*, **40**(5-6), 4109-4128.

Eringen, A.C. (1983), "On differential equations of nonlocal elasticity and solutions of screw dislocation and surface waves", *J. Appl. Phys.*, **54**(9), 4703-4710.

Eringen, A.C. (2002), *Nonlocal Continuum Field Theories*, Springer-Verlag, New York, USA.

Eringen, A.C. and Edelen, D.G.B. (1972), "On nonlocal elasticity", *Int. J. Eng. Sci.*, **10**, 233-248.
Fang, B., Zhen, Y.X., Zhang, C.P. and Tang, Y. (2013), "Nonlinear vibration analysis of double-walled carbon nanotubes based on nonlocal elasticity theory", *Appl. Math. Modell.*, **37**(3), 1096-1107.
Gibson, R.F., Ayorinde, E.O. and Wen, Y.F. (2007), "Vibrations of carbon nanotubes and their composites: A review", *Compos. Sci. Technol.*, **67**, 1-28.
Harris, P.J.F. (2009), *Carbon Nanotube Science*: *Synthesis*, *Properties and Applications*, Cambridge University Press, UK.
Hassan, I.H.A.H. (2002), "On solving some eigenvalue problems by using a differential transformation", *Appl. Math. Comput.*, **127**, 1-22.
Hassan, I.H.A.H. (2008a), "Application to differential transformation method for solving systems of differential equations", *Appl. Math. Modell.*, **32**, 2552-2559.
Hassan, I.H.A.H. (2008b), "Comparison differential transformation technique with Adomian decomposition method for linear and nonlinear initial value problems", *Chaos*, *Solitons Fractals*, **36**, 53-65.
He, X.Q., Kitipornchai, S. and Liew, K.M. (2005a), "Buckling analysis of multi-walled carbon nanotubes: a continuum model accounting for van der Waals interaction", *J. Mech. Phys. Solids*, **53**(2), 303-326.
He, X.Q., Kitipornchai, S., Wang, C.M. and Liew, K.M. (2005b), "Modeling of van der Waals force for infinitesimal deformation of multi-walled carbon nanotubes treated as cylindrical shells", *Int. J. Solids Struct.*, **42**(23), 6032-6047.
Hsiao, K.T., Alms, J. and Advani, S.G. (2003), "Use of epoxy/multiwalled carbon nanotubes as adhesives to join graphite fibre reinforced polymer composites", *Nanotechnol.*, **14**, 791-793.
Huang, D.J., Ding, H.J. and Chen, W.Q. (2007), "Analytical solution for functionally graded magneto-electro-elastic plane beams", *Int. J. Eng. Sci.*, **45**(2), 467-485.
Iijima, S. (1991), "Helica microtubes of graphitic carbon", *Nature*, **354**, 56-58.
Ke, L.L., Xiang, Y., Yang, J. and Kitipornchai, S. (2009), "Nonlinear free vibration of embedded double-walled carbon nanotubes based on nonlocal Timoshenko beam theory", *Comput. Mater. Sci.*, **47**(2), 409-417.
Khare, R. and Bose, S. (2005), "Carbon nanotube based composites-A review", *J. Miner. Mater. Character. Eng.*, **4**(1), 31-46.
Li, C., Thostenson, E.T. and Chou, T.W. (2008), "Sensors and actuators based on carbon nanotubes and their composites: A review", *Compos. Sci. Technol.*, **68**, 1227-1249.
Pan, E. and Han, F. (2005), "Exact solution for functionally graded and layered magneto-electro-elastic plates", *Int. J. Eng. Sci.*, **43**(3), 321-339.
Pour, H.R., Vossough, H., Beygipoor, M.M.H.G. and Azimzadeh, A. (2015), "Nonlinear vibration analysis of a nonlocal sinusoidal shear deformation carbon nanotube using differential quadrature method", *Struct. Eng. Mech., Int. J.*, **54**(6), 1061-1073.
Pradhan, S.C. (2012), "Nonlocal finite element analysis and small scale effects of CNTs with Timoshenko beam theory", *Finite Elem. Anal. Des.*, **50**, 8-20.
Reddy, J.N. (2007), "Nonlocal theories for bending, buckling and vibration of beams", *Int. J. Eng. Sci.*, **45**(2-8), 288-307.
Reddy, J.N. (2010), "Nonlocal nonlinear formulations for bending of classical and shear deformation theories of beams and plates", *Int. J. Eng. Sci.*, **48**(11), 1507-1518.
Reddy, J.N. and Pang, S.D. (2008), "Nonlocal continuum theories of beams for the analysis of carbon nanotubes", *J. Appl. Phys.*, **103**(2), 023511.
Reissner, E. (1984), "On a certain mixed variational theory and a proposed application", *Int. J. Numer. Methods Eng.*, **20**(7), 1366-1368.
Reissner, E. (1986), "On a mixed variational theorem and on a shear deformable plate theory", *Int. J. Numer. Methods Eng.*, **23**(2), 193-198.
Ru, C.Q. (2000), "Effect of van der Waals forces on axial buckling of a double-walled carbon nanotube", *J. Appl. Phys.*, **87**(10), 7227-7231.
Shakouri, A., Lin, R.M. and Ng, T.Y. (2009), "Free flexural vibration studies of double-walled carbon nanotubes with different boundary conditions and modeled as nonlocal Euler beams via the Galerkin

method", *J. Appl. Phys.*, **106**(9), 094307.
Sladek, J., Sladek, V., Krahulec, S., Chen, C.S. and Young, D.I. (2015), "Analyses of Circular Magnetoelectroelastic plates with functionally graded material properties", *Mech. Adv. Mater. Struct.*, **22**(6), 479-489.
Thai, H.T. (2012), "A nonlocal beam theory for bending, buckling, and vibration of nanobeams", *Int. J. Eng. Sci.*, **52**, 56-64.
Thai, H.T. and Vo, T.P. (2012), "A nonlocal sinusoidal shear deformation beam theory with application to bending, buckling, and vibration of nanobeams", *Int. J. Eng. Sci.*, **54**, 58-66.
Thostenson, E.T., Ren, Z. and Chou, T.W. (2001), "Advances in the science and technology of carbon nanotubes and their composites: a review", *Compos. Sci. Technol.*, **61**, 1899-1912.
Vinayan, B.P., Nagar, R., Raman, V., Rajalakshmi, N., Dhathathreyan, K.S. and Ramaprabhu, S. (2012), "Synthesis of graphene-multiwalled carbon nanotubes hybrid nanostructure by strengthened electrostatic interaction and its lithium ion battery application", *J. Mater. Chem.*, **22**, 9949-9956.
Wang, C.M., Tan, V.B.C. and Zhang, Y.Y. (2006a), "Timoshenko beam model for vibration analysis of multi-walled carbon nanotubes", *J. Sound Vib.*, **294**(4-5), 1060-1072.
Wang, C.M., Zhang, Y.Y., Ramesh, S.S. and Kitipornchai, S. (2006b), "Buckling analysis of micro- and nano-rods/tubes based on nonlocal Timoshenko beam theory", *J. Phys. D: Appl. Phys.*, **39**(17), 3904-3909.
Wu, C.P. and Lai, W.W. (2015a), "Reissner's mixed variational theorem-based nonlocal Timoshenko beam theory for a single-walled carbon nanotube embedded in an elastic medium and with various boundary conditions", *Compos. Struct.*, **122**, 390-404.
Wu, C.P. and Lai, W.W. (2015b), "Free vibration of an embedded single-walled carbon nanotube with various boundary conditions using the RMVT-based nonlocal Timoshenko beam theory and DQ method", *Physica E*, **68**, 8-21.
Wu, C.P. and Lee, C.Y. (2001), "Differential quadrature solution for the free vibration analysis of laminated conical shells with variable stiffness", *Int. J. Mech. Sci.*, **43**, 1853-1870.
Wu, C.P. and Tsai, Y.H. (2007), "Static behavior of functionally graded magneto-electro-elastic shells under electric displacement and magnetic flux", *Int. J. Eng. Sci.*, **45**(9), 744-769.
Wu, C.P., Hong, Z.L. and Wang, Y.M. (2017), "Geometrically nonlinear static analysis of an embedded multiwalled carbon nanotube and van der Waals interaction", *J. Nanomech. Micromech.-ASCE*, **7**, 04017012 (12 pages).
Yalcin, H.S., Arikoglu, A. and Ozkol, I. (2009), "Free vibration analysis of circular plates by differential transformation method", *Appl. Math. Comput.*, **212**, 377-386.
Yang, J., Ke, L.L. and Kitipornchai, S. (2010), "Nonlinear free vibration of single-walled carbon nanotubes using nonlocal Timoshenko beam theory", *Physica E*, **42**(5), 1727-1735.

CC